



1

2

*Geophysical Research Letters*

3

Supporting Information for

4

**Interaction of Saturn's Hexagon with convective storms**

5

6

**A. Sánchez-Lavega<sup>1,\*</sup>, E. García-Melendo<sup>2</sup>, R. Hueso<sup>1</sup>, T. del Río-Gaztelurrutia<sup>1</sup>, A. Simon<sup>3</sup>,  
M. H. Wong<sup>4</sup> K. Ahrens-Velásquez<sup>2</sup>, M. Soria<sup>2</sup>, T. Barry<sup>5</sup>, C. Go<sup>6</sup>, C. Foster<sup>7</sup>**

7

8

9

<sup>1</sup> Departamento Física Aplicada I, Escuela de Ingeniería de Bilbao, Universidad del País Vasco  
UPV/EHU, Bilbao, Spain.

10

11

12

<sup>2</sup> Universitat Politècnica de Catalunya UPC, Terrasa, Spain

13

14

<sup>3</sup> NASA Goddard Space Flight Center/690, Greenbelt, MD, USA

15

16

<sup>4</sup> University of California, Berkeley, CA, USA

17

18

<sup>5</sup> Broken Hill Observatory, Broken Hill, Australia

19

20

<sup>6</sup> University of San Carlos, Cebu, Philippines

21

22

<sup>7</sup> Astronomical Society of Southern Africa, Centurion, South Africa

23

24

Corresponding author: Agustín Sánchez-Lavega (agustin.sanchez@ehu.eus)

25

26

27

28

**Contents of this file**

29

30

Text S1 to S3

31

32

Figures S1 to S5

33

34

Tables S1 to S2

35

36

37

38

39

40

36 **Text S1.**

37 Table S1 gives the list of observers and their instrumentation whose images have been used in  
 38 this study. The full list of observers contributing with their images of Saturn in 2019 and 2020  
 39 appear in the databases:

40  
 41 ALPO-Japan: <http://alpo-j.asahikawa-med.ac.jp/Latest/Jupiter.htm>

42 PVOL (Planetary Virtual Observatory Laboratory): <http://pvol2.ehu.eus/pvol2/search/form>

43

44 **Table S1**

45 Instruments descriptions: SC stands for Schmidt Cassegrain, DK for Dall-Kirkham Cassegrain,

46 RC Ritchey-Chretien, (\*) Chilescope (<http://www.chilescope.com/>)

47

48

Observer	Country	Telescope	Filters	Days
Luis Amiama Gómez	Santo Domingo	SC 280 mm	R,G,B	1
Ecleido WS. Azevedo	Brazil	Newton 300mm	R,G,B	5
Christofer M. Baez	Santo Domingo	Newton 203mm	R,G,B	3
Trevor Barry	Australia	Newton 408mm	R,G,B,CH4	281
Joaquin Camarena	Spain	SC 355mm	R,G,B, CH4	2
Andy Casely	Australia	SC 355mm	R,G,B,CH4	10
Ethan Chappel	USA	SC 203mm	R,G,B	2
Jean-Luc Dauvergne	France	DK 250mm	L,R,G,B	4
Darren Ellemor	Singapore	SC 280mm	R,G,B	1
Pericles Enache	Brazil	SC 203mm	R,G,B	1
Clyde Foster	South Africa	SC 355mm	R,G,B, CH4	76
Christopher Go	Philippines	SC 355mm	R,G,B,CH4	56
Satoshi Ito	Japan	Newton 250mm	R,G,B	1
Teruaki Kumamori	Japan	SC 355 mm	L,R,G,B	5
George Lamy	USA	SC 355mm	R,G,B	1
Mark Lonsdale	Australia	SC 280mm	R,G,B	1
Bruce MacDonald	USA	SC 355mm	L,R,G,B	8
Niall MacNeill	Australia	SC 355mm	R,G,B,CH4	28
Walter Martins	Brazil	Newton 203mm Newton 305mm	R,G,B	6
Lucas Magalhaes	Brazil	Newton 317mm	R,G,B	1
Phil Miles	Australia	Newton 508mm	R,G,B, CH4	2
Masaaki Nagase	Japan	SC 235mm	R,G,B	1
Tiziano Olivetti	Thailand	DK 505mm	R,G,B	20
Damian Peach	Chile (*)	RC 1000mm	R,G,B	12
Christophe Pellier	France	SC 305mm	R,G,B	1
Darryl Pfintzer Milika	Australia	SC 355mm	R,G,B	6
Vlamiir da Silva	Brazil	SC 203mm	R,G,B	1
Avani Soares	Brazil	SC 355mm	L,R,G,B	12
Maciel B. Sparrenberger	Brazil	Newton 317mm	R,G,B	1
Vicenzo della Vecchia	Italy	Cassegrain 300mm	R,G,B	1
Leandro Yasutake	Argentina	Newton 355mm	R,G,B	1
Kenkichi Yunoki	Japan	Newton 260mm	R,G,B	1
Anthony Wesley	Australia	Newton 508mm	R,G,B,CH4	4
Michael Wong	Australia	Newton 305mm	R,G,B, CH4	26

49 **Text S2.**

50

51 Description of the analysis of ground-based and HST images. The images submitted by the  
 52 observers to the databases were normally, reprocessed for contrast enhancement, navigated  
 53 for limb determination and measured. We used the WinJUPOS software (Hahn & Jacquesson  
 54 <http://www.grischa-hahn.homepage.t-online.de/>) to navigate the images transforming the  
 55 original pixel coordinates of a point on Saturn's disk to longitude and latitude positions over the  
 56 planet. This software was also employed to produce polar stereographic maps. For the  
 57 determination of the longitudes on the planet disk we use System III (period = 9 hr 55 min 29.711  
 58 s) (Archinal et al. 2018).

59

60 **Text S3.**

61

62 We provide here details of the numerical dynamical SW model we have used. The polar storm  
 63 was simulated using the Shallow Water model (SW) where the weather layer is modeled as a  
 64 thin sheet of homogeneous fluid. SW models are a simplification of the real atmosphere, but  
 65 still they preserve a good deal of the large scale dynamics on a rotating sphere or ellipsoid, while  
 66 allowing a fast computation by explicitly integration of the prognostic variables. Our SW is a  
 67 parallelized code able to run on supercomputers. Model resolution was 0.02 degrees per control  
 68 volume and the time step was set to 1 second, which ensured that the CFL condition was not  
 69 violated. The storm was modeled as a continuous mass injection throughout the whole  
 70 simulation time. Simulations were run for a Rossby radius of deformation  
 71  $L_R = (gD)^{1/2} / f \sim 300 \text{ km}$ , where  $g \cong 10 \text{ m s}^{-2}$ ,  $D = 1000 \text{ m}$  is the depth of the model, and  
 72  $f \cong 3.2 \times 10^{-4} \text{ s}^{-1}$  is the Coriolis parameter. Saturn's zonal winds were continuously forced as  
 73 described in García-Melendo and Sánchez-Lavega (2017).

74

75

76

77

**Table S2. Shallow Water model simulations: parameter space ranges**

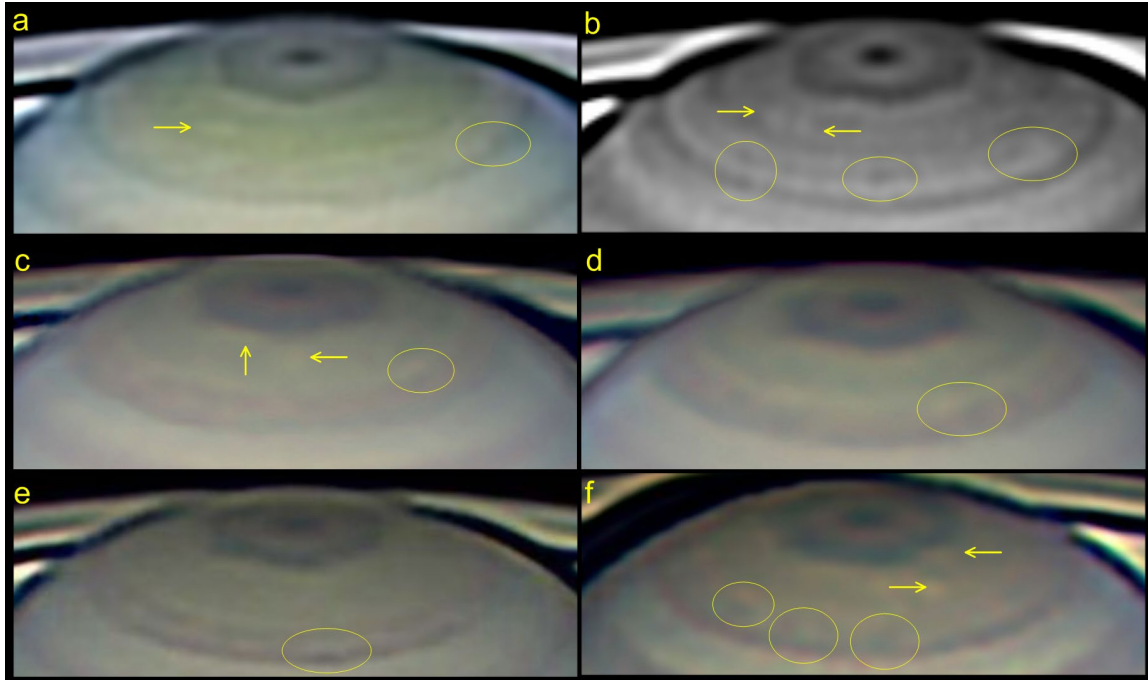
<i>Parameter</i>	<i>Value or range of values</i>
Horizontal resolution	$\Delta x = \Delta y = 0.05 \text{ deg pix}^{-1}$
Time step	1 second
Layer depth	1000 m
Simulation domain (long, lat)	Long [0°, 180°]; Lat [63°, 83°]
Storm major and minor semiaxes dimensions	1° × 1°
Latitude range	73.0 to 77.0 in 0.5 deg steps
Continuous mass flow injection Q range	$1 \times 10^8 \text{ to } 1 \times 10^{12} \text{ m}^3 \text{ s}^{-1}$
Number of simulations	50

78

79

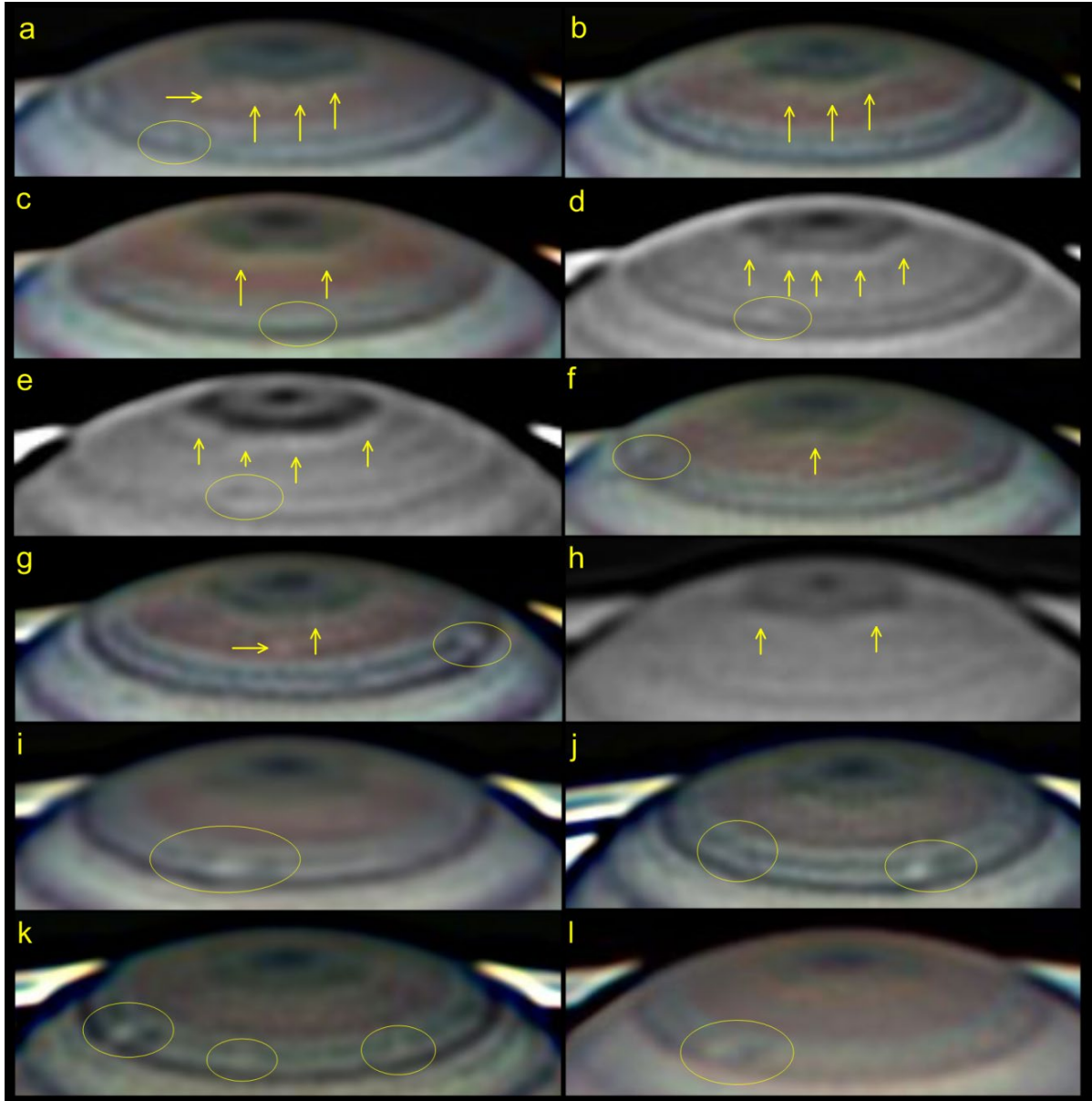
80

81



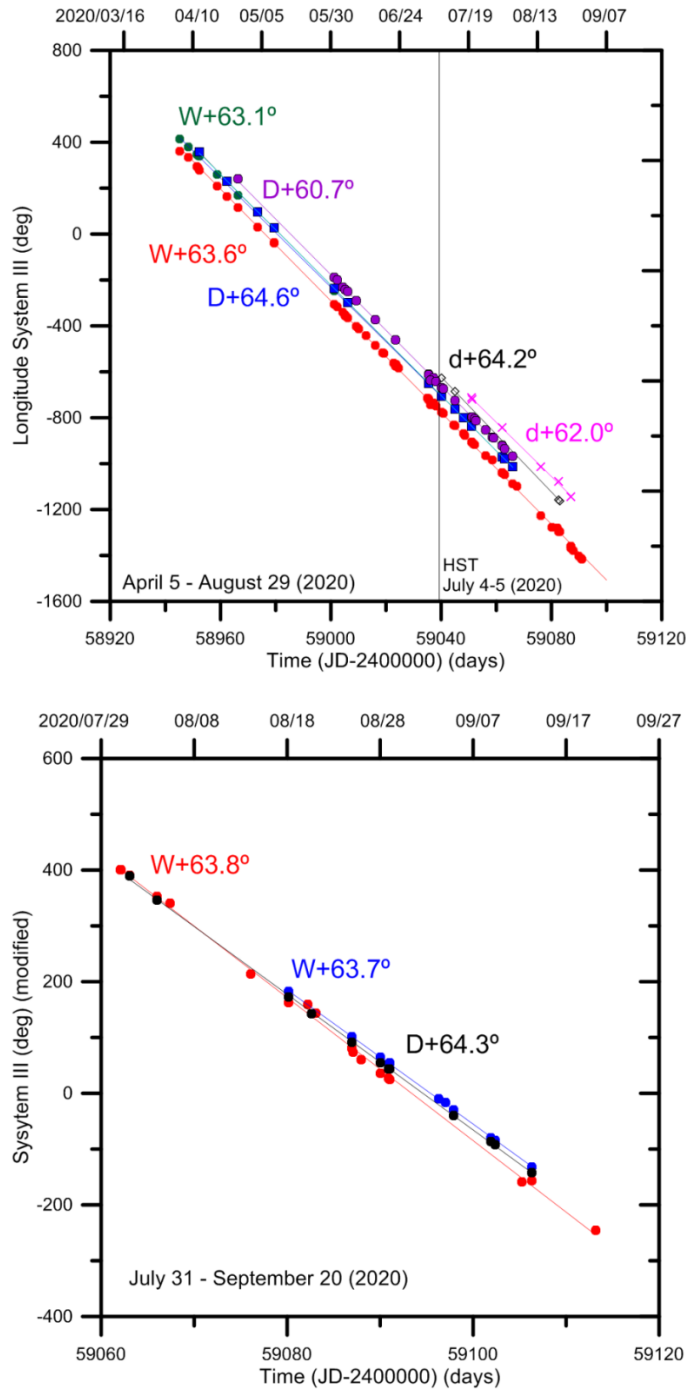
82  
 83  
 84  
 85  
 86  
 87  
 88  
 89  
 90  
 91

**Figure S1.** Color composite images of the North Polar Region of Saturn in 2019. The hexagon wave is easy to identify and the lower dark belt locates at latitude 60°N. The arrows mark the spots at the hexagon southern edge and in close latitudes. The circles enclose long-lived spots tracked along the year as shown in Figure S3. Dates and observers: (a) 8 April 10:23UT, D. Peach; (b) 20 April 21:03 UT, T. Olivetti; (c) 25 April 19:49 UT, N. MacNeill; (d) 27 April 18:09 UT, N. MacNeill; (e) 24 May 18:14, N. MacNeill; (f) 15 September 12:13 UT, N. MacNeill.



92  
93  
94  
95  
96  
97  
98  
99  
100  
101  
102  
103  
104

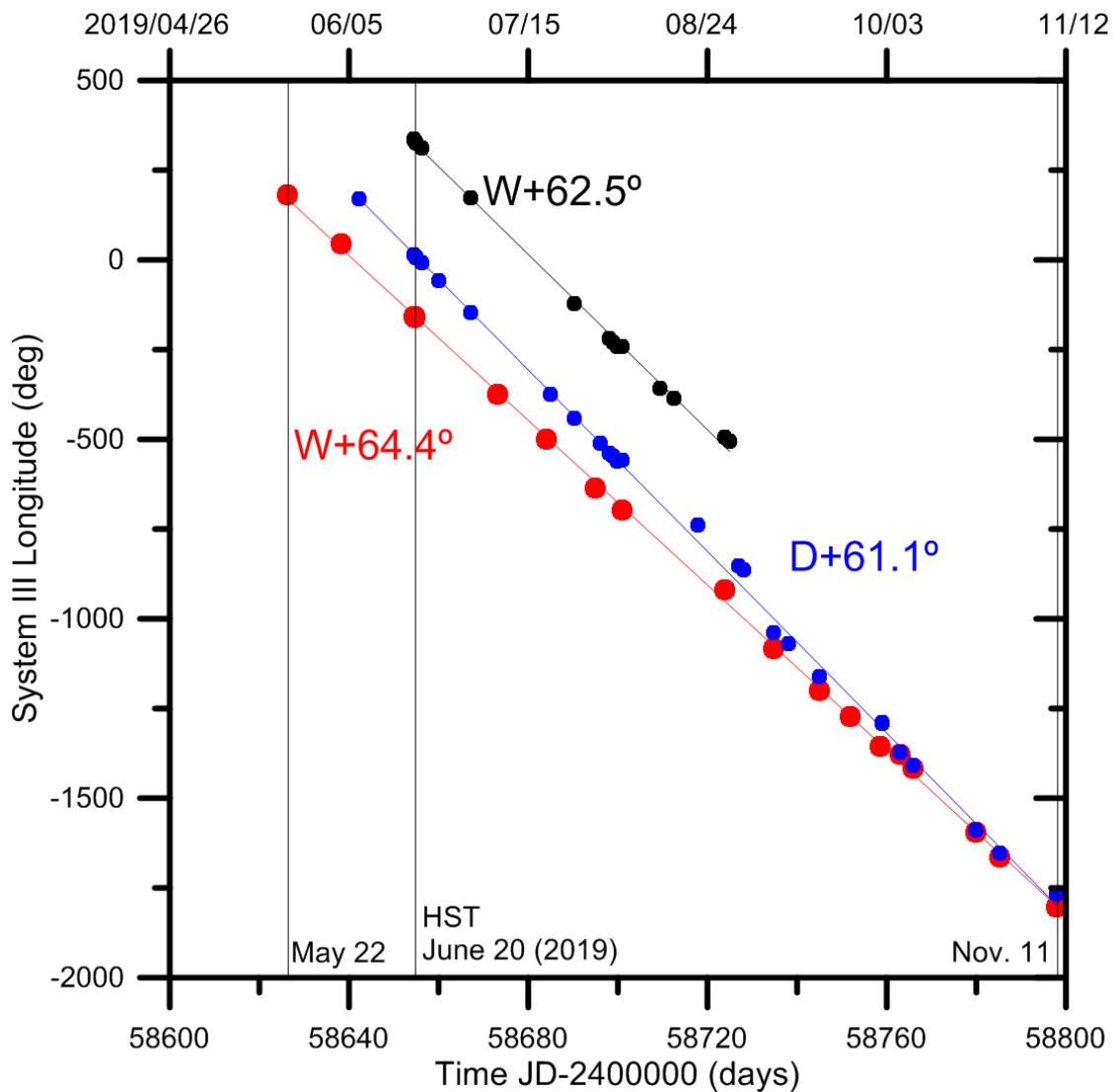
**Figure S2.** Color composite images of the North Polar Region of Saturn in 2020. The hexagon wave is easy to identify in (a-h) due to the combination of filters used. The lower dark belt locates at latitude  $60^{\circ}\text{N}$ . The arrows mark the spots at the hexagon southern edge (latitudes  $75^{\circ}\text{N}$ - $76^{\circ}\text{N}$ ) and in close latitudes. The circles enclose long-lived spots tracked along the year as shown in Figure S4. Dates and observers: (a) 9 May 20:20 UT, C. Go; (b) 11 May 30:34 UT, C. Go; (c) 12 May 20:00 UT, C. Go; (d) 15 May 20:48 UT, T. Olivetti; (e) 16 May 21:48 UT, T. Olivetti; (f) 27 May 18:39 UT, C. Go; (g) 8 June 18:35 UT, C. Go; (h) 6 July 15:01 UT, T. Barry; (i) 9 July 17:26 UT, C. Go; (j) 17 July 15:33 UT, C. Go; (k) 20 July 14:41 UT, C. Go; (l) 31 July 13:41 UT, N. MacNeill.



105  
 106  
 107  
 108  
 109  
 110  
 111  
 112  
 113  
 114

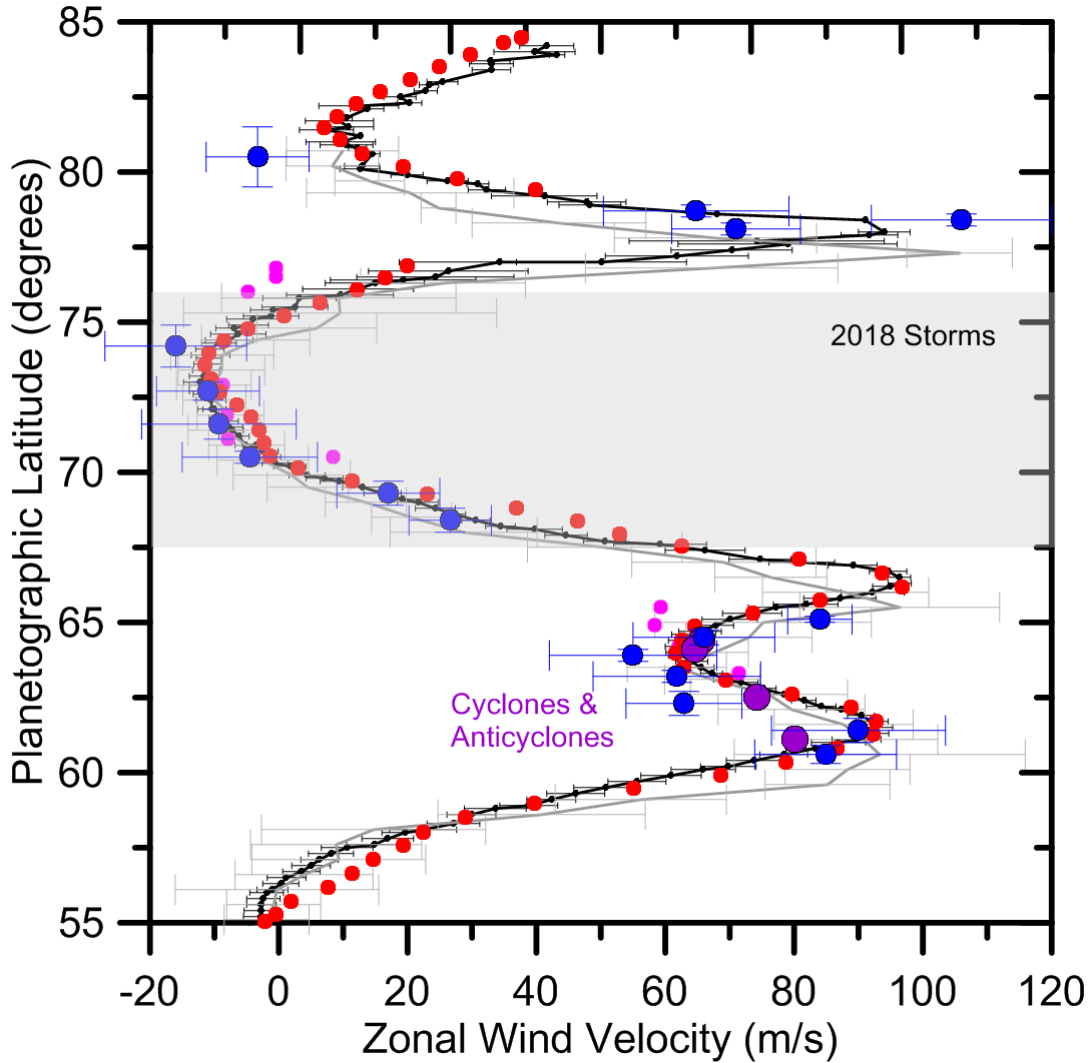
**Figure S3.** Long-term drift in System III longitudes during 2020 of various large white (W) and dark (D) spots and smaller dark spots (d) observed at red wavelengths ( $\sim 650 - 900$  nm) on the double jet between latitudes  $\sim 60^\circ\text{N}$  and  $67^\circ\text{N}$ . The W and D spots form a system of cyclones and anticyclones as described in del Rio-Gaztelurrutia et al. (2018). The planetographic latitudes of the spots are indicated. Their velocities in the wind profile are shown in Figure 2. The upper x-axis gives the date (year/month/day).

115



116  
 117  
 118  
 119  
 120  
 121  
 122  
 123  
 124  
 125  
 126  
 127

**Figure S4.** Long-term drift in System III longitudes during 2019 of three white (W) and dark (D) spots observed at red wavelengths ( $\sim 650 - 900$  nm) on the double jet between latitudes  $\sim 60^\circ\text{N}$  and  $67^\circ\text{N}$ . These spots form a system of cyclones and anticyclones as described in del Rio-Gaztelurrutia et al. (2018). The planetographic latitudes are indicated. Their velocities in the wind profile are drawn in Figure S5. The upper x-axis gives the date (year/month/day).



128  
 129  
 130  
 131  
 132  
 133  
 134  
 135  
 136  
 137  
 138  
 139  
 140  
 141

**Figure S5.** Zonal wind profile in Saturn's North Polar Region measured in 2019 relative to System III rotation frame. The red dots are from the correlation velocimetry on HST images in 19-20 June 2019 (Simon et al., 2021) and blue dots from motions of major features manually tracked and binned in latitude bands with a width  $0.5^\circ - 1^\circ$  from the same HST images (error bars indicated). The magenta dots are spots tracked in ground-based images in 2019. The three large purple dots correspond to the long-lived spots (Figs. S1 and S3). The black profile and dark dots is the wind profile from Cassini ISS measurements [García-Melendo et al. 2011] and the grey profile from Voyagers 1 and 2 [Sánchez-Lavega et al. 2001]. The shadowed area indicates the latitude band where the 2018 storms evolved.